Int. J. Adv. Eng. Pure Sci. 2024, 36(2): <134-139>
DOI: 10.7240/jeps.1314336

RESEARCH ARTICLE / ARAŞTIRMA MAKALESİ

Synthesis, Structural Characterization and Temperature Effects on Chloroform Vapor Sensing Properties of ZnO Nanocrystals

Doruk YILDIZTEKİN [1], **Fatih DUMLUDAĞ** [1]
[1] *Marmara University, Faculty of Science, Department of Physics, 34722, Kadıköy/İstanbul, TÜRKİYE*

Abstract
In this study, nanocrystalline ZnO were synthesized onto glass substrates by using sol-gel method. Structural characterizations were performed by XRD, SEM and AFM techniques. Potential application of nanocrystal ZnO as chloroform sensor was investigated. Response of the fabricated thin films of the ZnO nanocrystals towards chloroform vapor was investigated depending on gas concentration (750-15000 ppm) between the temperatures of 22–150 ºC in nitrogen ambient. Gas flow rates were controlled by using flow controller and flow meters. All the measurement system was computerized.
XRD results revealed that thin film of the ZnO nanocrystals on the glass substrate was in crystal form and can be characterized by 036-1451 JCPDS number. Crystallite sizes of the ZnO nanocrystals were determined both by SEM images and the Scherrer equation. The crystallite sizes were calculated between 27.9 – 50.4 nm using the Scherrer equation. The sensors showed reversible response towards the chloroform vapor in the measured temperature and gas concentration range. Response time and sensitivity values of the sensors towards the chloroform vapor were also calculated. The increase in temperature caused to increase in sensitivity values. The best sensitivity values were obtained at 150 °C.
Keywords: XRD, SEM, AFM, Sensor, Chloroform, Nano.

I. INTRODUCTION

Volatile organic compounds (VOCs) are organic liquids and can be found indoor air due to wood polishes, paints, adhesives and so on. VOCs vapor are hazardous and can cause long-term health and environmental problems even at ppm concentration levels. Chloroform ($CHCl_3$) is one of the VOCs and colorless liquid. Previously, chloroform was used as an inhalation anesthetic in surgeries, but it is not used in this way, nowadays. It was reported that by the ATSDR (Agency for Toxic Substances and Disease Registry) in a group of 1502 people (exposure less than 22 500 ppm), dose-related bradycardia developed in 8% of the peoples, and cardiac arrhythmia developed in 1.3% of the peoples [1]. A number of studies, using different sensing materials, were reported to sense the chloroform vapor previously due to importance of the sensing the chloroform vapor [2, 3, 4].

Some electrical parameters such as resistance and impedance of some metal oxide semiconductors changes when the materials exposed to gases. ZnO based gas sensors are used frequently in order to detect toxic and harmful gases because of its physicochemical properties [5, 6]. ZnO is a wide band gap metal oxide material and takes place between semiconductors and ionic materials [7, 8]. Several techniques have been reported to deposit doped and undoped ZnO films such as vapor condensation, thermal evaporation, spray pyrolysis, magnetron sputtering, metal organic chemical vapor deposition, and sol-gel [9, 10, 11, 12, 13].

ZnO based sensors are usually operated at elevated temperatures but it has been studied rarely at low temperatures below 200 ºC and even at room temperature [14]. In this study ZnO nanocrystal structures have synthesized onto the glass substrate using sol-gel method. Digitated gold electrodes were deposited onto the nanocrystalline film in thermal evaporation system then the sensor was tested towards chloroform vapor at different gas concentrations and temperatures. The sensors were found reversible. Sensitivity of the sensors increased with increasing temperature. The best sensitivity values were obtained at 150 ºC.

II. MATERIALS and METHOD

Glass substrates were cleaned using general cleaning procedures in order to synthesize ZnO nanocrystals onto glass substrates. To do this, the glass substrates were washed with isopropyl alcohol, acetone and DI-water in

Corresponding Author: Fatih DUMLUDAĞ, **Tel:** 0216 777 33 09, **E-mail:** fatihdumludag@marmara.edu.tr
Submitted: 14.06.2023, **Revised:** 24.03.2024, **Accepted:** 26.03.2024

ultrasonic cleaner with 15 minutes periods at 50 ºC. The cleaned glass substrates were then dried by nitrogen blow and heated at 90 ºC for one hour.

Thin films of ZnO were deposited onto the cleaned glass substrates using sol-gel spin coating route. Precursor solution was first prepared. To prepare the precursor solution 10 cc methanol was used as solvent. Appropriate amount of zinc acetate dihydrate ($Zn(CH_3COO)_2$ $.2H_2O$) is slowly added to solvent while the solvent is mixed by using magnetic stirrer at 700 rpm and left to stir for 5 minutes. After that 0.4 cc diethanolamine (DEA) ($HN(CH_2CH_2OH)_2$ and 0.5 cc of DI-water water was added drop by drop. The solution was then left to stir for 3 hours. The solution was spin coated at 2000 rpm onto the glass substrate by using spinner MODEL 6700 SERIES followed by annealing at 125 °C for 15 minutes. The solution was deposited onto the glass substrate 12 times by using the procedure explained above. Final annealing was performed at 600 °C for 2.5 hours.

Chemical sensors are devices that convert a chemical state into an electrical signal. In order to get electrical signal corresponding to chemical state, a suitable transducer is required to detect a gas molecule. ZnO nanocrystals deposited glass substrates were placed into thermal evaporation system in order to fabricate transducer. 20 couples interdigitated gold electrodes (IDE) were deposited onto the ZnO nanocrystal film in high vacuum ambient (10^{-6} mbar) by using a shadow mask. Thickness of the gold electrodes was kept at 2000 Å by using film thickness monitor. Schematic diagram of the IDE was presented in Figure 1.

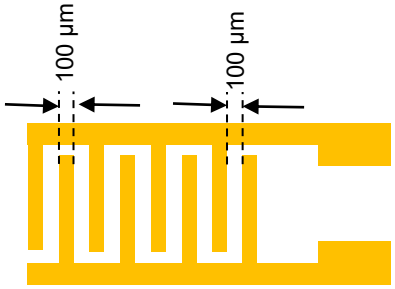

Figure 1. Schematic diagram of the transducer

Structural characterizations of the ZnO nanocrystals were performed by XRD, SEM, and AFM techniques. XRD measurements were performed by using Bruker D8 Advance with characteristic wavelength of 1.54059 Å. SEM and AFM images were obtained by using Digital Instruments NanoScope IV, and Philips XL 30 S, respectively. Crystallite size of the ZnO nanocrystals were calculated by using Scherrer formula (Equation 1).

$$L = \frac{K\lambda}{\beta Cos\theta} \quad \textbf{(1)}$$

where, L is the crystallite size, K is the dimensionless shape factor, (0.94), λ is the wavelength of the x-ray in nm, β is the full width half maximum of the peak (FWHM) in radians, and θ is the Bragg angle in radians.

The fabricated ZnO nanocrystals-based sensor was placed in homemade Teflon gas test chamber in order to determine response of the sensor towards chloroform vapor. The chamber was placed in a sealed chemical hood. Chloroform vapor were produced in washing bottle filled with extra pure grade chloroform from MERCK. Concentration of the vapor was calculated using Antoine equation. High purity nitrogen gas used as carrier gas and total flow rate was kept at 100 cc/min. Flow rates were controlled by using the MKS gas flow controller and gas flowmeters. Gas sensing measurements were performed depending on gas concentration at different temperatures between 22 ºC - 150 ºC. Sensitivity and response time values of the sensors, which is defined as the time it takes to reach 90% of the total change in measured gas concentration, were also calculated.

III. RESULTS and DISCUSSION

3.1. Structural Characterization

Structure of the ZnO were studied by XRD, SEM and AFM techniques. Figure 2 shows XRD pattern of the ZnO structure deposited onto glass substrates. The results revealed that the ZnO films were in crystal form. XRD results are matched with the pattern of ZnO JCPDS number 036-1451. Crystallite size of the ZnO nanocrystals were calculated by using Scherrer formula (Equation 1). The calculations revealed that the crystallite size varies between 27.9 – 50.4 nm. The 2θ degrees given in the XRD pattern were presented in Table 1.

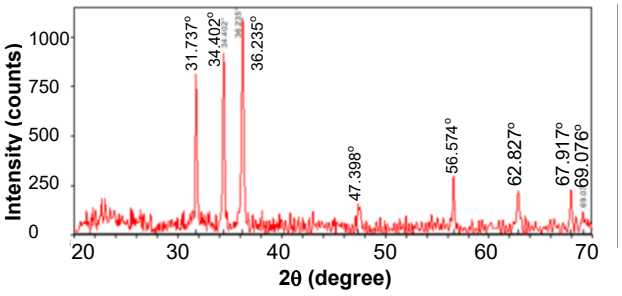

Figure 2. XRD pattern of the synthesized nanocrystalline ZnO film.

Table 1. 2θ degrees obtained from XRD pattern of the synthesized ZnO nanocrystals.

2θ values of the peaks (in degrees)	31.737	34.402	36.235	47.398	56.574	62.827	67.917	69.076
Miller Indices	(100)	(002)	(101)	(102)	(110)	(103)	(112)	(201)

SEM images of the ZnO nanocrystals with (×20000) and (×50000) magnification which is deposited onto glass substrate were shown in Figure 3. The image was obtained by using SEM operated at 15 kV. As can be seen from the Figure the particles are distributed homogeneously and the particles have a round shape. Different crystallite sizes were observed in SEM images, and their sizes varied between 24.8 – 101.0 nm. This may be because some particles within the particle may have agglomerated over time. As a result, it can be seen that the average ZnO nanocrystallite size calculated from the XRD data with the Scherrer formula is also supported by the SEM image.

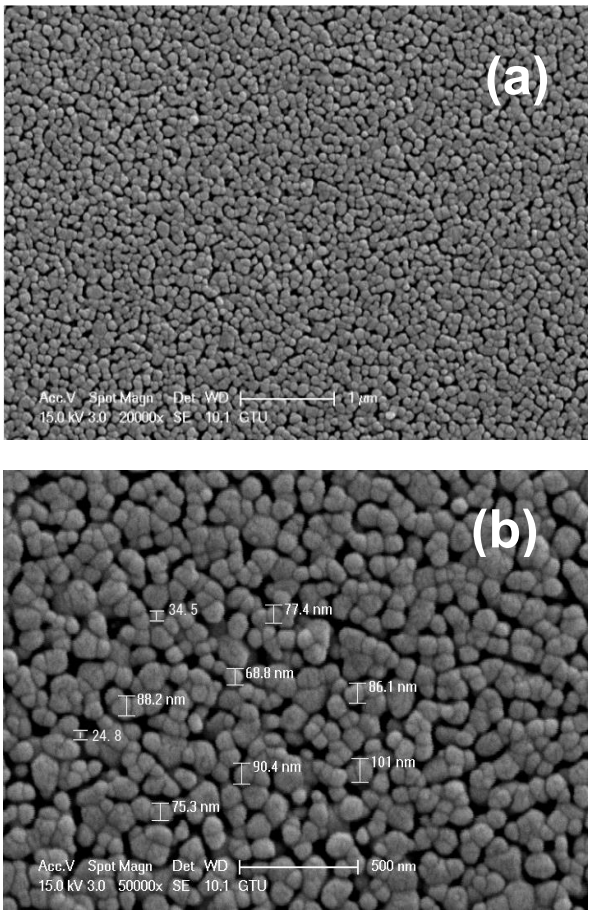

Figure 3. SEM images of the synthesized nanocrystalline ZnO film deposited onto glass substrate. (a) magnification (×20000) (b) magnification (×50000)

3D AFM images of the ZnO nanocrystal film of 2 μm × 2 μm and 5 μm × 5 μm size were presented in Figure 4. From the AFM images roughness was determined about 4.30 nm by the AFM software program.

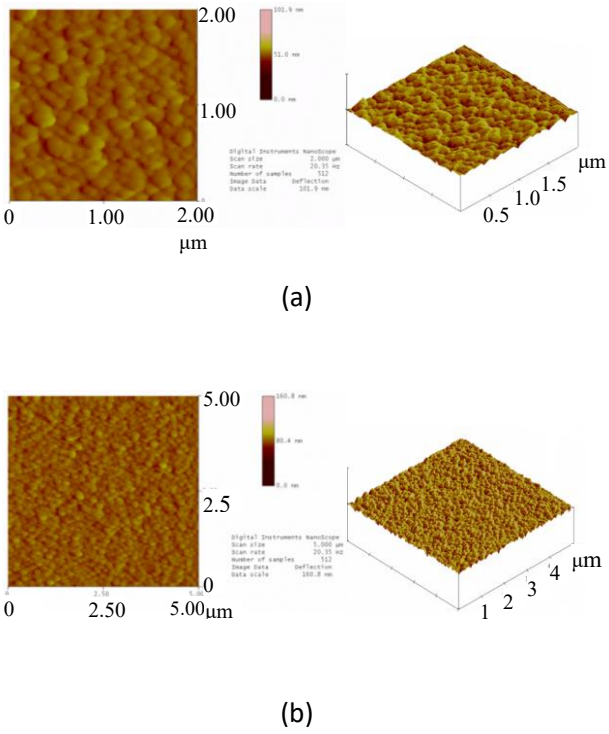

Figure 4. 3D AFM images of the synthesized nanocrystalline ZnO film deposited onto glass substrate
(a) 2 μm x 2 μm (b) 5 μm x 5 μm.

3.2. Gas Sensing Properties

Gas sensing measurements were conducted in homemade Teflon gas test chamber. Chloroform vapor and nitrogen gas were used as target gas and carrier gas, respectively. In order to test the sensor towards chloroform vapor, the gas sensing measurements were performed depending on gas concentration (750, 2 250, 3 750, 7 500, and 15 000 ppm) at different temperatures between 22 ºC–150 ºC. Chloroform vapor were produced in washing bottle filled with extra pure grade chloroform from MERCK. Gas concentrations were calculated by using Antoine equation given below (Equation 2).

$$Log_{10}P = A - \frac{B}{(T+C)} \quad \textbf{(2)}$$

where P is the vapor pressure in bar, T is the temperature in Kelvin, A, B, and C are vapor depended parameters. Response of the sensor were examined by recording the current values, which is passing through the sensor, as a function of time (Current-time (I–t)) at different gas concentrations and temperatures. Figure 5a shows the real-time response of the ZnO based sensor towards chloroform vapor at room temperature.

By examining the Figure 5a, before the chloroform vapor (target gas) exposure to sensor, current passing through the sensor nearly remains same under the flow of nitrogen gas (carrier gas). There is no remarkable change in current before the sensor is exposed towards to chloroform vapor. After the target gas flow turned on, the current begins to increase and then rate of increase slows down. In the 300 seconds time interval, the sensor response does not reach to saturation. After the target gas flow turned off, the current begins to decrease and current passing through the sensor decreases nearly to the initial current value during the sensor exposed to carrier gas. It was observed that total time needed to decrease the initial current value takes greater than 300 seconds. Because of this behavior it can be concluded that the response of the sensor were reversible. As it is well known, adsorption process occur while a sensor exposed to a target gas molecules. During this process if an electron is transferred from the target gas to n-type sensing material of the sensor, the conductivity of the sensing material is increased (physisorption). The increase in conductivity cause an increase in current passing through the sensor [15, 16]. We may conclude that the increase in current passing thorough the our sensor arises from the electron transfer from chloroform to ZnO film due to adsorption process. Another observation is that the change in current passing through the sensor is increased with an increase in gas concentration from 750 ppm to 15000 ppm. We may conclude that change in current increases with increasing gas concentration, since the number of electrons transferred from the target gas to sensing material is proportional to target gas concentration [15, 16, 17].

Response of the sensor at elevated temperatures were presented in Figure 5b (at 100 ºC) and Figure 5c (at 150 ºC). The sensor showed similar behavior with that of the response at room temperature. The sensor also showed reversible behavior at all measured temperature range and gas concentrations.

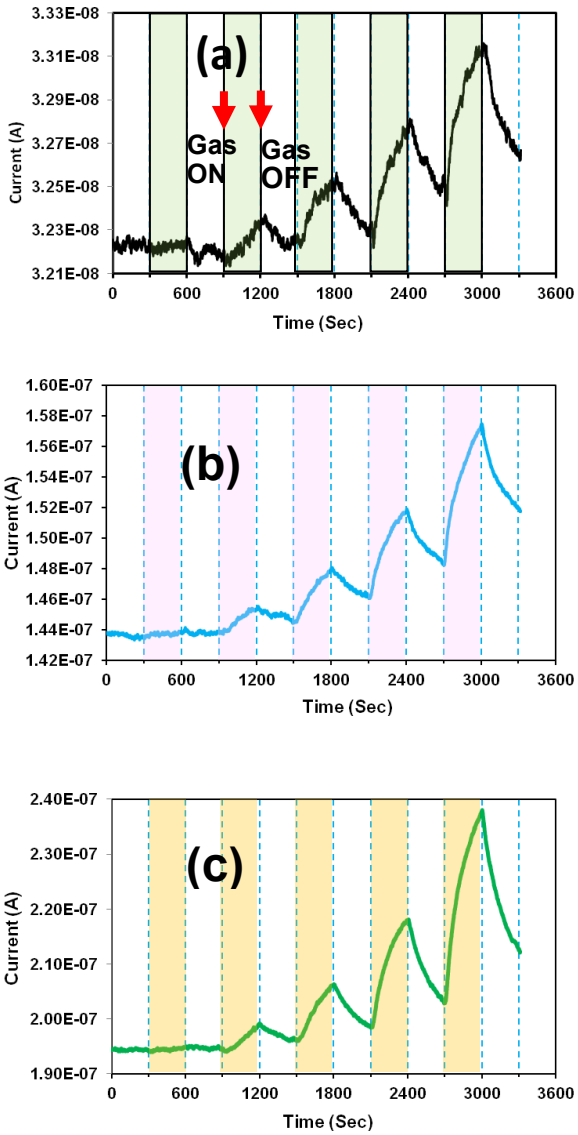

Figure 5. Response of the ZnO nanocrystal film towards chloroform vapor at (a) 22 ºC (room temperature, RT) (b) 100 ºC (c) 150 ºC.

Response time values (τ_{90}) of the sensors was defined as the time it takes to reach 90% of the total change in current in the measured gas concentration. Calculated response time values of the sensors as a function of chloroform vapor concentrations were presented in Figure 6. By examining the Figure 6 it can be seen clearly that, in general, increase in gas concentration caused to decrease in response time values.

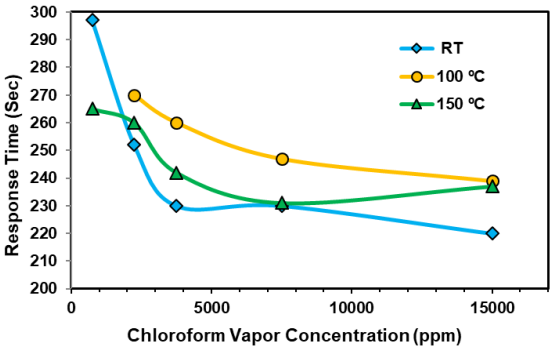

Figure 6. Response time values of the ZnO nanocrystal film as a function of gas concentration at indicated temperatures.

Sensitivity is defined as:

$$S = \left[\frac{\Delta I}{I_o} \right] \quad (3)$$

where I_o is the current passing through the sensor at the time the sensor exposed to target gas, ΔI is the change in current passing through the sensor corresponding to gas concentration.

Sensitivity values of the sensors were presented in Figure 7. The results showed that sensitivity of the ZnO nanocrystal film increased with increasing chloroform vapor concentration. Additionally, increment in temperature caused an increase in sensitivity also.

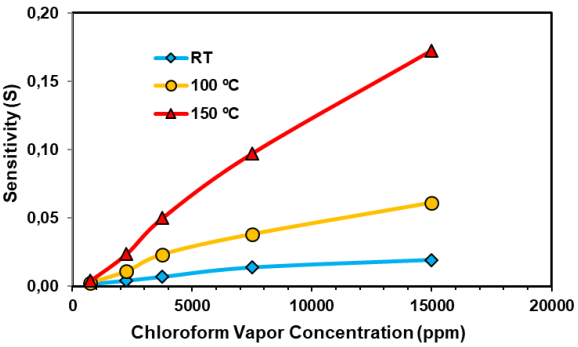

Figure 7. Sensitivity of the ZnO nanocrystal film as a function of gas concentration at indicated temperatures.

IV. CONCLUSION

ZnO nanocrystals were fabricated onto glass substrates. The XRD pattern revealed that the ZnO films were in crystal form and matched with the pattern of ZnO JCPDS number 036-1451. The crystallite sizes of ZnO nanocrystals were determined by the Scherrer formula, varying between 27.9 – 50.4 nm. Gas sensing measurements showed that the ZnO based sensors can be used as chloroform vapor sensor successfully between the chloroform vapor concentrations of 750 – 15 000 ppm even at room temperature. The results were also showed that sensitivity of the sensors were increased with increasing temperature from 22 °C to 150 °C. Sensing mechanism of the sensors can be explained by electron exchange between the ZnO nanocrystals and chloroform vapor while the adsorption occurs on the surface of the ZnO. Since ZnO shows n-type semiconducting property we can conclude that an electron is transferred from chloroform to ZnO film and that causes an increase in dc conductivity of the ZnO film (physisorption). The best sensitivity values were obtained at 150 ºC.

ACKNOWLEDGMENT

This work was supported by Research Fund of Marmara University with the project number: FYL-2022-10636. The authors gratefully acknowledge the Marmara University Commission of Scientific Research Projects (BAPKO) for this partial financial support.

REFERENCES

[1] https://www.atsdr.cdc.gov/ToxProfiles/ tp6-c2.pdf

[2] Çimen, Y., Ermiş, E., Dumludağ, F., Özkaya, A.R., Salih, B. ve Bekaroğlu, Ö. (2014). Synthesis, characterization, electrochemistry and VOC sensing properties of novel ball-type dinuclear metallophthalocyanines. Sensors and Actuators B 202 1137–1147.

[3] Franco, M.A., Conti, P.P., Andre, R.S. ve Correa, D.S. (2022) A review on chemiresistive ZnO gas sensors. Sensors and Actuators Reports., 4 100100.

[4] Ren, X., Xu, Z., Liu, D., Li, Y., Zhang, Z. ve Tang, Z. (2022) Conductometric NO_2 gas sensors based on MOF-derived porous ZnO nanoparticles. Sensors and Actuators B: Chemical., 357 131384.

[5] Kang, Y., Yu, F., Zhang, L., Wang, W., Chen, L. ve Li, Y. (2021) Review of ZnO-based nanomaterials in gas sensors. Solid State Ionics., 360, 115544.

[6] Zhang, J., Wang, S., Wang, Y., Xu, M., Xia, H., Zhang, S., Huang, W., Guo, X. ve Wu, S. (2009) ZnO hollow spheres: Preparation, characterization, and gas sensing properties. Sensors and Actuators B., 139 411–417.

[7] Kim, K.K., Kim, H.S, Hwang, D.K., Lim, J.H. ve Park, S.J. (2003) Realization of p-type ZnO thin films via phosphorus doping and thermal

activation of the dopant. Applied Physics Letters., vol. 83 (1) 63–65.

[8] Srivastava, A.K., Chakraborty, B.R. ve Chandra, S. (2009) Crystallographically oriented nanorods and nanowires of rfmagetron- sputtered zinc oxide. Journal of Nanomaterials., vol. 2009, Article ID 310360.

[9] Grassi, M., Soares, D.A.W., De Queiroz, A.A.A., Bressiani, A.H.A. ve Bressiani, J.C., (2004) Organometallic chemical vapor deposition of compound semiconductors. Materials Science and Engineering B., vol. 112, no. 2-3, pp. 179–181.

[10] Al Asmar, R., Ferblantier, G., Mailly, F., Gall-Borrut, P. ve Foucaran, A. (2005) Effect of annealing on the electrical and optical properties of electron beam evaporated ZnO thin films. Thin Solid Films., vol. 473, no. 1, 49–53.

[11] Kang, D, J., Kim, J.S., Jeong, S.W., Roh, Y., Jeong, S.H. ve Boo, J.H. (2005) Structural and electrical characteristics of R.F. magnetron sputtered ZnO films. Thin Solid Films,. vol. 475, no. 1-2, 160–165.

[12] Cheng, X.L., Zhao, H., Huo, L.H., Gao, S. ve Zhao, J.G. (2004) ZnO nanoparticulate thin film: preparation, characterization and gas-sensing property. Sensors and Actuators B., vol. 102, no. 2, 248–252.

[13] Sbrockey, N.M. ve S. Genesan. (2004) ZnO thin films by MOCVD. III-Vs Review., vol. 17, no. 7, 23–25.

[14] Wang, L., Kang, Y., Liu, X., Zhang, S., Huang, W. ve Wang, S. (2002) ZnO nanorod gas sensor for ethanol detection. Sensors and Actuators B., 162, 237-243.

[15] Şenoğlu S., Özer M., Dumludağ F., Acar N., Salih B., Bekaroğlu Ö., (2020) Synthesis, characterization, DFT study, conductivity and effects of humidity on CO_2 sensing properties of the novel tetrakis-[2-(dibenzylamino)ethoxyl] substituted metallophthalocyanines, Sensors and Actuators B: Chemical, vol. 310, 127860

[16] Köksoy B., Aygün M., Çapkın A., Dumludağ F., Bulut M., (2018) Electrical and gas sensing properties of novel cobalt(II), copper(II), manganese(III) phthalocyanines carrying ethyl 7-oxy-4,8-dimethylcoumarin-3-propanoate moieties, Journal of Porphyrins and Phthalocyanines, vol. 22, 1-16

[17] Yasemin Ç., Emel E., Dumludağ F., Özkaya A., Salih B., Bekaroğlu Ö., (2014) Synthesis, characterization, electrochemistry and VOC sensing properties of novel ball-type dinuclear metallophthalocyanines, Sensors and Actuators B: Chemical, vol. 202, 1137-1147